

## GAIN AND NOISE THEORETICAL ANALYSIS OF $\text{Er}^{3+}$ - DOPED $\text{Ti:LiNbO}_3$ STRAIGHT WAVEGUIDE AMPLIFIERS

B. SAVU, Georgiana C. CONSTANTIN, N. N. PUȘCAȘ\*

*În această lucrare este prezentată o analiză a câștigului și a figurii de zgomot care caracterizează amplificatoarele optice integrate drepte de tip  $\text{Er}^{3+}$ :  $\text{Ti:LiNbO}_3$ . Deducerea formulelor câștigului spectral optic, a cifrei spectrale optice de zgomot și a raportului semnal-zgomot, respectiv evoluția acestor parametri a fost făcută în aproximația de câștig mic ținând seama de suprapunerea dintre profilul distribuțiilor radiațiilor de pompaj, semnal și dopantului (ionii de  $\text{Er}^{3+}$ ). În simulările efectuate s-a considerat că profilul ionilor de  $\text{Er}^{3+}$  este de tip erfc, gaussian sau constant pe lățimea ghidului și gaussian în adâncime, cu o concentrație la suprafață de  $7 \cdot 10^{25} \text{ m}^{-3}$  și o adâncime de difuzie de  $20 \mu\text{m}$ . Simulările evidențiază evoluția parametrilor menționați mai sus pentru diferite regimuri de pompaj și lungimi ale ghidurilor optice de undă. Rezultatele simulărilor pot fi utilizate la proiectarea circuitelor optice integrate dopate cu ionii pământurilor rare.*

*In this paper we report a theoretical analysis of the gain and noise figure which characterize the  $\text{Er}^{3+}$ -doped  $\text{Ti:LiNbO}_3$  straight waveguide amplifiers. The derivation and the evaluation of the spectral optical gain, the spectral noise figure and the signal-to-noise ratio were performed under the small gain approximation taking into account the overlap between the pump, signal and dopant ( $\text{Er}^{3+}$  ions) distribution profiles. In our simulations the  $\text{Er}^{3+}$ -profile is considered erfc, Gaussian or constant in depth and Gaussian in width, with a surface concentration of about  $7 \cdot 10^{25} \text{ m}^{-3}$  and a diffusion depth of  $20 \mu\text{m}$ . The simulations show the evolution of these parameters under various pump regimes and waveguide lengths. The obtained results can be used for the design of complex rare earth doped integrated circuits.*

**Keywords:** Spectral gain, spectral noise figure, signal-to-noise ratio, single and double pass,  $\text{Er}^{3+}$ -doped  $\text{Ti:LiNbO}_3$  straight waveguide amplifiers

---

\*Drd., Prep., Prof., Physics Department, University "Politehnica" of Bucharest, ROMANIA

## Introduction

The theoretical study of the optical amplification plays an important role in obtaining integrated amplifiers having low noise and high optical gain. In the last years, a great attention has been devoted to the analysis of the spectral optical gain and noise of Er doped fibres and waveguide amplifiers taking into account the overlap between the pump, signal and dopant distribution profiles. [1-4].

The work already done in the analysis of optical fiber amplifiers [1] was used in the elaboration of the theoretical models which describe the optical amplification in waveguides [2]-[4]. In this paper, we proposed a novel technique for evaluating the spectral optical gain, the spectral noise figure, the signal to noise ratio (SNR) and the amplified spontaneous emission (ASE) photon number of straight  $\text{Er}^{3+}$ -doped  $\text{Ti:LiNbO}_3$  waveguide amplifiers.

The structure of the paper is as follows. In Section 2, we present the basic equations which describe the optical amplification in waveguides, and the expressions of the above mentioned parameters. Section 3 is devoted to the numerical implementation and to the discussion of the simulation results. Then Section 4 proposes a conclusion to this work.

### 1. Theoretical considerations

The amplification in straight  $\text{Er}^{3+}$ -doped  $\text{Ti:LiNbO}_3$  waveguide amplifiers is described using a quasi-two-level model under the small gain approximation in the wavelength range  $1.44 \mu\text{m} < \lambda < 1.64 \mu\text{m}$  [1]-[4]. The system of coupled first order differential equations in the case of the two-level model for the upper population level  $N_2(x, y, z)$  and the optical power spectral components  $P_{km}^\pm(z)$  with the frequency  $\nu_k$  at the longitudinal coordinate  $z$  has the form:

$$N_2(x, y, z) = N_{T0}d(x, y) \frac{\sum_{k,m} \frac{\tau}{h\nu_k} \sigma_{a,km} (P_{km}^+(z) + P_{km}^-(z)) i_m(x, y)}{1 + \sum_{k,m} \frac{\tau}{h\nu_k} (\sigma_{a,km} + \sigma_{e,km}) (P_{km}^+(z) + P_{km}^-(z)) i_m(x, y)} \quad (1)$$

$$\begin{aligned} \frac{d}{dz} P_{km}^\pm(z) = & \pm \left\{ \left[ (\sigma_{e,km} + \sigma_{a,km}) \int_A N_2(x, y, z) i_{km}(x, y) dx dy \right] P_{km}^\pm(z) \right\} \pm \\ & \left\{ - \left[ (\sigma_{a,km} \int_A N_T(x, y, z) i_{km}(x, y) dx dy + \alpha_{km}) \right] P_{km}^\pm(z) \right\} \pm \quad (2) \\ & \left\{ h\nu_k \Delta \nu_k \sigma_{e,km} \int_A N_2(x, y, z) i_{km}(x, y) dx dy \right\} \end{aligned}$$

where  $P_{km}^{\pm}(z)$  represent the power longitudinal distribution of the field component at frequency  $\nu_k$ , having the polarization denoted by the index  $m$  ( $m$  being  $\pi$  for the parallel or  $\sigma$  for the perpendicular directions to the optical axis of the crystal) in the forward (+) and backward (-) propagation directions; the normalized transversal intensity distribution  $i_{km}(x, y)$  has been considered wavelength independent. The scattering losses of the integrated optical waveguides have been taken into account by the term  $\alpha_{km}$ .

In Eq. (2), the term  $h\nu_k\Delta\nu$  represents an equivalent spontaneous emission input noise power in the frequency slot  $\Delta\nu$  corresponding to the frequency  $\nu_k$ .

The dopant concentration can be written in terms of surface concentration  $N_{T_0}$  and normalised dopant distribution  $d(x, y)$ . Therefore:  $N_T(x, y) = N_{T_0}d(x, y)$ . In Eqs (1), (2) the expressions

$$\Gamma_{Tm}(z) = \int_A d(x, y) i_m(x, y) dx dy \quad (3)$$

$$\Gamma_{2m}(z) = \frac{1}{N_{T_0}} \int_A N_2(x, y, z) i_m(x, y) dx dy \quad (4)$$

represent the overlap integrals between the normalized field intensity and the (normalized) dopant distribution ( $\Gamma_{Tm}$ ) and the (normalized) upper laser level population ( $\Gamma_{2m}$ ) presented in fig. 1 for TE and TM polarisations. In our simulations the Er<sup>3+</sup>-profile is considered erfc, Gaussian or constant in depth and Gaussian in width.

Taking into account the *photon statistics master equation*, Eqs. (1), (2) of the linear amplifier and the theoretical model presented in papers [1] and [4] we calculated the the spectral optical gain, the spectral noise figure, and the amplified spontaneous emission photon number

$$G(z, \nu) = \exp\left\{\int_0^z [\gamma_e(z', \nu) - \gamma_a(z', \nu) - \alpha(\nu)] dz'\right\} \quad (5)$$

$$N(z, \nu) = G(z, \nu) \int_0^z \frac{\gamma_e(z', \nu)}{G(z', \nu)} dz' \quad (6)$$

represent the spectral gain and the ASE photon number, respectively.

In order to study the behaviour of the noise in the optical amplifier one defined an optical signal-to-noise ratio, (*SNR*) can be defined as follows:

$$\begin{aligned}
SNR_0(z) &= \frac{\langle \langle n(z) \rangle - \langle n(z) \rangle_{ASE} \rangle_T^2}{\sigma^2(z)} \\
&= G^2(z) \langle n(0) \rangle^2 / \left( G(z) \langle n(0) \rangle + N(z) + 2G(z)N(z) \langle n(0) \rangle + N^2(z) \right) \quad (7)
\end{aligned}$$

where  $\langle \dots \rangle_T$  represents the time average over the bit period (bit rate  $B = 1/T$ ) and  $\sigma^2(z) = \langle n^2(z) \rangle - [\langle n(z) \rangle]^2$  the noise power measured over this period [1].

A measure of the *SNR* degradation experienced by the signal after passing through the amplifier is characterized by the amplifier optical noise figure,  $F_0(z)$  defined by the relation:

$$F_0(z) = \frac{SNR_0(0)}{SNR_0(z)} \quad (8)$$

where  $SNR_0(0)$  represents the optical *SNR* at the amplifier input. In the case of large gain (i. e.  $G(z) \gg 1$ ) the noise figure is given by [1]:

$$F_0(z, \nu) = \frac{1 + 2N(z, \nu)}{G(z, \nu)} \quad (9)$$

where the term  $2N/G$  correspond to a beat noise regime at the peak gain and the term  $1/G$  to a shot noise at the spectrum tails. In deriving the relations of the signal-to-noise ratio and noise figure at the input and output of the device (Eqs. (5)-(9)) we considered an input signal with Poisson statistics ( $\sigma^2(0) = \langle n(0) \rangle$ ).

## 2. Discussion of the simulation results

The simulations are performed under the small gain approximation using a Runge-Kutta formula (4 th order, 4 stages) as the basic integration method with an iterative procedure [3], [4].

A particular care should be taken for the evaluation of  $\Gamma_{2m}$  because this quantity determines the incremental gain in Eqs. (5) and depends on the actual value of the approximation for  $P_{km}^\pm(z)$ ; this imply that at each step of the forward and backward integration along  $z$ , we have to evaluate the integral  $\Gamma_{2m}$ . Because of our choice of a Runge-Kutta formula (4 th order, 4 stages) as the basic integration method, at each step we should evaluate four time (one for each stage)

the overlap integral, within a large expense of computer time. Therefore, we decided to perform the transversal integration only at the first stage at each step, and to use the computed value also for the other three stages; this approximation appears not to have a great influence on the solution and represents a good compromise between accuracy and computation time.

The intensity profiles  $i_m(x, y)$  used in the evaluation of  $\Gamma_{2m}(z)$  (fig. 1) and  $\Gamma_{Tm}(z)$  are introduced in the model as a set of measured values, while the dopant distribution  $d(x, y)$  is approximated by Gaussian or *erfc* functions in depth ( $y$ ) and constant in width ( $x$ ). These profiles correspond to different diffusion conditions or crystal fabrications. An *erfc* profile is obtained when the diffusion of the Er<sup>3+</sup> ions is not completed, while a Gaussian profile corresponds to case where all the Er ions have diffused into the crystal. The last case (constant in depth) corresponds to the case where the crystal is doped with Er<sup>3+</sup> during the growth process.

The computer simulations for the evaluation of the statistical properties of Er<sup>3+</sup>-doped LiNbO<sub>3</sub> waveguide amplifiers have been performed using the parameters found from literature [2]-[5]. We assumed a 1484 nm pump and a signal at  $\lambda=1531$  nm, having 1  $\mu$ W input power.

The Er<sup>3+</sup>-profile has been considered Gaussian in depth and constant in width, with a surface concentration of about  $7 \cdot 10^{25} \text{ m}^{-3}$  and a diffusion depth of 20  $\mu\text{m}$  [4]. The waveguide length is assumed to be  $L=5.4$  cm when not specified; the pump and signal input reflectivity always is  $R(0)=0$  while the output is  $R(L)$ .

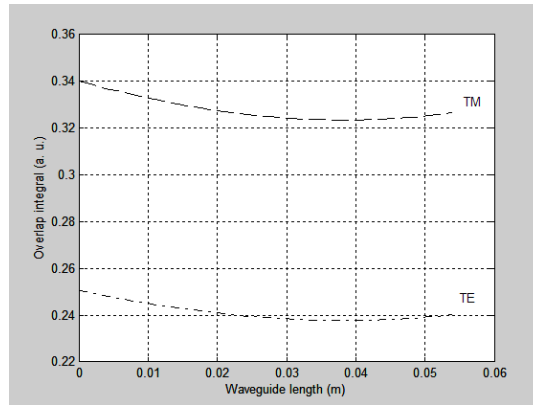


Fig. 1. The overlap integral  $\Gamma_{2m}$  vs waveguide length.

The small signal gain  $G(z) = \ln[P_{signal}(z)/P_{signal}(0)]$  for the single pass configuration, is presented in Fig. 2 for the input pump power of 150 mW (high pump regime) and of 25 mW (low pump regime) and of 1  $\mu$ W for signal. At a high input pump power levels of  $P(0) = 150$  mW (exceeding the transparency or threshold pump power  $P_{th} = 18.5$  mW for the single pass and  $P_{th} = 12.5$  mW for the double pass configuration of the optical amplifier) the gain evolution in single pass configuration is linear up to waveguide lengths of the order  $\sim 10$  cm (fig. 3). The simulation results are in good agreement with other theoretical predictions and experimental results [2], [3].

Also, we have calculated numerically the spectral dependence of the gain, amplified spontaneous emission photon number, noise figure and  $SNR$  for a single pass but also for double pass configuration of the optical amplifier with signal and pump wavelengths of 1531 nm and 1484 nm, respectively.

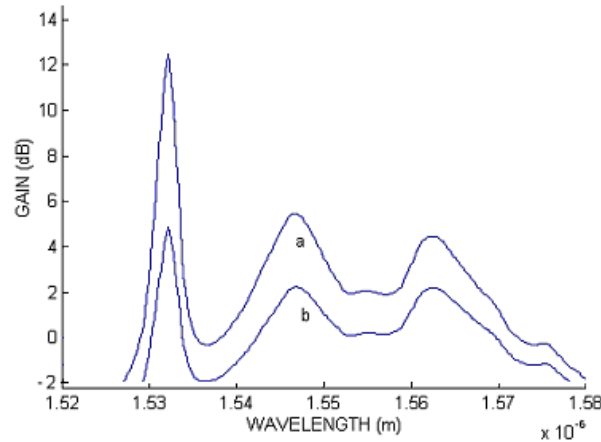


Fig. 2. Spectral gain behaviour: a)  $P(0) = 150$  mW and b)  $P(0) = 25$  mW;  $L = 5.4$  cm.

As can be seen (Fig. 4), the calculated noise figure values for  $\text{Er}^{3+}$ -doped  $\text{LiNbO}_3$  waveguides amplifiers in double pass and high pump regime are comparable at peak values (7.8 dB for  $\lambda = 1531$  nm) with those obtained in optical  $\text{Er}^{3+}$ -doped fiber amplifiers.

When the waveguide is pumped a few times above the threshold (i. e.  $P(0) = 50$  mW) the forward and backward noise figure spectra are very similar, the forward noise figure power being lower about 5 % at peak values than the backward noise figure power, as was showed [1] for the optical fiber amplifiers case. In the high pump regime, however, the difference between forward and

backward noise figure vanishes. The same effect was obtained for the ASE spectra.

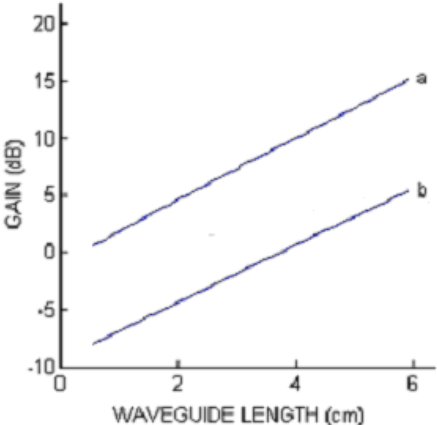


Fig. 3. The optical gain vs waveguide length: a)  $P(0) = 150$  mW and b)  $P(0) = 25$  mW.

The double pass *SNR* spectra are presented in Fig. 5 in the above mentioned conditions; the spectra show minima around 1531 nm.

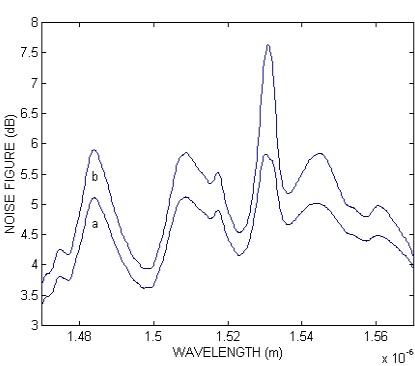


Fig. 4. The spectral noise figure: a)  $P(0) = 150$  mW and b)  $P(0) = 25$  mW.

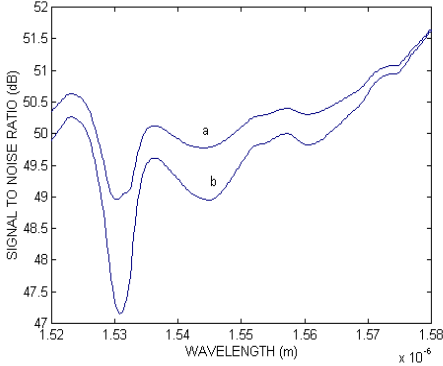


Fig. 5. The spectral signal-to-noise ratio: a)  $P(0) = 150$  mW and b)  $P(0) = 25$  mW.

In an interval of 2 nm around  $\lambda = 1531$  nm the double pass configuration with high pump regime ( $P(0) = 150$  mW) allows to obtain high gain (about 14.5 dB) and low noise figures (5.9 dB) for an  $\text{Er}^{3+}$ -doped  $\text{LiNbO}_3$  waveguides amplifier of 5.4 cm length.

We have also investigated the dependence of the above mentioned parameters on the pump power in the range 25-150 mW in single pass (Figs. 6, 7), but also in double pass configurations, high gains and low noise figures being available in high pump regimes and double pass configuration.

When computing the evolution of the noise figure as a function of the waveguide length in the range 1-10 cm for single pass configuration we observe that this parameter increases to rather high values, about 5.5 dB in Fig. 8, for single pass configuration and it tends to saturate.

### Conclusions

In this paper we present a theoretical analysis and an accurate evaluation of the spectral optical gain, spectral noise figure and  $SNR$  for an  $\text{Er}^{3+}$ -doped  $\text{LiNbO}_3$  waveguide amplifier pumped at 1484 nm with a TE pump.

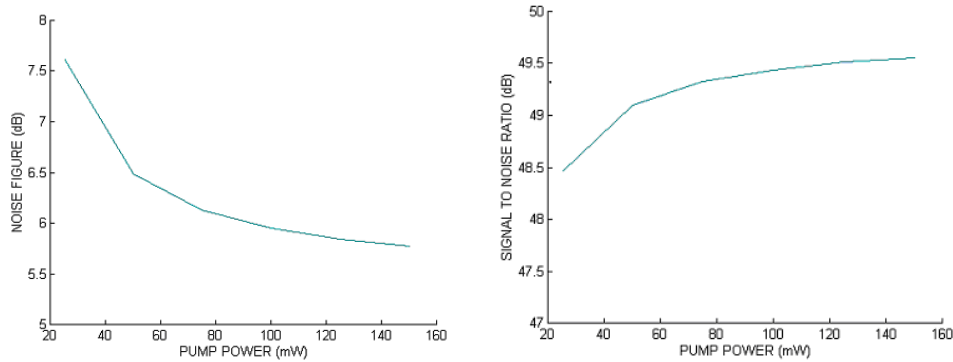


Fig. 6. The spectral noise figure vs pump power. Fig. 7. The signal-to-noise ratio vs pump power.

The theoretical analysis was made using the small gain approximation in the unsaturated pump regime for both single and double pass configurations. From the behaviour of the above mentioned parameters under various pumping regimes and waveguide lengths we demonstrated that high gains and low noise figures are achievable in high pump regimes and double pass configuration.



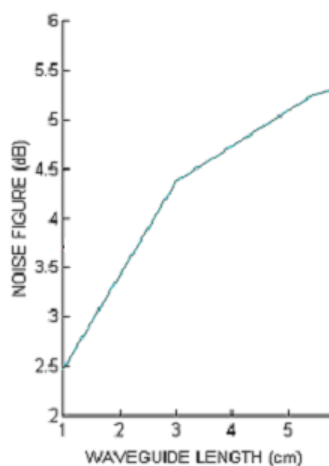


Fig. 8. The optical noise figure vs waveguide length in the high pump regime  $P = 150$  mW and single pass configuration.

## REFERENCES

1. *E. Desurvire*, 1994, Erbium-Doped Fiber Amplifiers (New York: Wiley).
2. *I. Baumann, R. Brinkmann, M. Dinand W. Sohler and S. Westenhofer*, Ti:Er:LiNbO<sub>3</sub> Waveguide Laser of Optimized Efficiency, IEEE J. Quant. Electr., QE-32, p. 1695-1706 (1996).
3. *M. Dinand, W. Sohler*, Theoretical Modeling of Optical Amplification in Er-doped Ti:LiNbO<sub>3</sub> Waveguides", IEEE J. Quant. Electr., QE-30, p. 1267-1276 (1994).
4. *N. N. Puscas, R. Girardi, D. Scarano, I. Montrosset*, Spectral noise analysis of single and double pass Er<sup>3+</sup>-doped LiNbO<sub>3</sub> waveguide amplifiers, Journal of Modern Optics, Vol. 45, No. 4, p. 847-859, (1998).
5. *N. N. Puscas*, Modelling and Evaluation of Some Spectroscopic Parameters of Er<sup>3+</sup>-Doped LiNbO<sub>3</sub> Optical Waveguides, SPIE, Vol. 5972, p. 308-318, (2005).